

1 Inverse determination of effective mechanical 2 properties of adhesive bondlines

3 Philipp Hass*, Falk K. Wittel, Miller Mendoza, Hans J. Herrmann, Peter Niemz

4 *Institute for Building Materials, ETH Zurich, Schafmattstrasse 6, 8093 Zurich,*
5 *Switzerland*

6 *Corresponding author:

7 +41 44 63 23250

8 +41 44 63 21174

9 phass@ethz.ch

10 **Abstract:** A new approach for determining the effective mechanical bondline properties
11 using a combined experimental-numerical modal analysis technique is proposed. After
12 characterizing clear spruce wood boards, an adhesive layer is applied on the boards'
13 surfaces. The shift of the eigenfrequencies resulting from the adhesive layer, together
14 with information about the bondline geometry can then be used to inversely determine the
15 mechanical properties of the adhesive layer using Finite Element Models. The calculated
16 values for clear wood, as well as for the adhesive layer lie within reasonable ranges, thus
17 demonstrating the method's potential.

18 Inverse Bestimmung von effektiven mechanischen Eigenschaften von 19 Klebfugen

20 **Zusammenfassung:** In dieser Arbeit wird eine neue Untersuchungsmethode zur
21 Bestimmung der effektiven mechanischen Eigenschaften von Klebfugen mittels
22 experimentell-numerisch kombinierter Modalanalyse vorgestellt. Die
23 Schwingungseigenschaften von Fichtenvollholzbrettern werden charakterisiert, bevor und
24 nachdem eine Klebstoffschicht auf die Holzflächen aufgebracht wird. Die durch die
25 Klebstoffschicht bedingte Änderung in den Eigenfrequenzen kann zusammen mit der
26 Klebfugegeometrie genutzt werden, um mittels Finiter Elemente Modelle, invers die
27 mechanischen Eigenschaften der Klebstoffschicht zu bestimmen. Das Potenzial der
28 vorgestellten Methode zeigt sich in den vielversprechenden Ergebnissen, die sowohl für
29 Vollholz, als auch für die Klebstoffschicht sinnvolle Werte annehmen.

30 **Keywords:** *modal analysis, bondline, FEM*

31 1. Introduction

32 Bonding of wood elements is of paramount importance for the production of
33 modern timber constructions. During the bonding process, adhesive penetrates
34 into the porous wood structure along all accessible pathways and, depending on
35 the adhesive properties, even into the micropores of the wood cell walls
36 (Suchsland 1958; Kamke and Lee 2007; Konnerth, Harper et al. 2008; Hass,
37 Wittel et al. 2011). Simplified, a wood-adhesive bond can be split into five stacked
38 layers consisting of pure adhesive in the center, an interphase of wood and cured
39 adhesive as well as two wood parts on the outermost (Habenicht 2006). For clear
40 wood, a vast amount of data is available (e.g. Kollmann and Cote 1968; Neuhaus
41 1981; Niemz 1993). The determination of the pure adhesive properties has been

42 subject to several investigations as well (Clad 1964; Konnerth, Jager et al. 2006;
43 Clauss, Dijkstra et al. 2011). In contrast, the interphase properties are almost
44 unknown. It can consist of entirely or partially adhesive filled tracheids, modified
45 cell walls and a composite with adhesive, and cell-wall fragments from the
46 production process. Nanoindentation was used to estimate the mechanical
47 properties of penetrated cell walls and adhesive filled lumen (Konnerth and Gindl
48 2006). Unfortunately nanoindentation only measures very local material
49 properties. For numerical models, however, it is necessary to have effective
50 properties that consider the influence of the hardened adhesive on the wood
51 properties, local defects due to curing stress such as cracks or voids (Hass,
52 Wittel et al. 2011), and geometric variations in a smeared way.

53 To identify the effective properties of the adhesive layer in the most mechanically
54 meaningful way, a non-destructive approach seems appropriate. Eigenfrequency
55 measurements have been used in the past to determine the properties of wood
56 boards and to identify changes in their mechanical properties (Berner, Gier et al.
57 2007). In this work we want to further exploit the potential of using changes in the
58 frequencies of certain eigenmodes to inversely identify the effective properties of
59 the adhesive layer, using finite element simulations. Eigenmode shifts can be
60 expected from the mass and effective properties of the adhesive layer as well as
61 modifications of wood properties in the interphase zone. As a minimal model, the
62 adhesive bond is simplified even further as a composition of only two layers with
63 distinct differences in their material behavior: Solid wood with its strong
64 orthotropic relationship between the three major directions, and a more or less
65 isotropic layer consisting of adhesive and wood adhesive interface.

66 **2. Material and Methods**

67 To determine the mechanical properties of the wood-adhesive interphase, an
68 inverse approach was chosen, in which experimental and numerical methods
69 were combined. In a first step, the mechanical properties of clear wood were
70 inversely determined. The procedure is repeated after an adhesive layer was
71 applied on the board. This way the affect of the adhesive layer on the
72 eigenfrequencies is maximized, while also avoiding warping of the samples. In
73 Figure 1a, the combined experimental and numeric procedure is schematized.

74 The spruce samples (*Picea Abies* (L.) Karst.) had the dimensions 320x125x5mm
75 with standing growth rings, as this orientation is expected to give the highest
76 frequency shifts when bending. This study is limited to urea-formaldehyde (UF),
77 since the typical massively cracked adhesive layer (see Figure 1b) should lead to
78 effective properties that differ significantly from those of the pure adhesive. Only
79 half of the amount of adhesive, recommended by the producers for one bondline
80 (200g/m²; solid content: 60%) was applied on each surface of the boards. To
81 ensure an even distribution of adhesive on the boards, a uniform film was applied
82 on a plastic sheet using an applicator with an adjustable slit (80µm). The sheets
83 were then placed on the board to assure instantaneous contact and pressed at
84 the recommended pressure of 0.7MPa. After curing, the samples were
85 acclimatized at 20°C, 65% relative humidity (RH). To visually determine the
86 bondline geometries, small samples were extracted and prepared for analysis

87 with an environmental scanning electron microscope. In Figure 1b a
88 representative image is shown with the highlighted interface between clear wood
89 and adhesive layer.

90

Figure 1

91 Literature values for the modulus of elasticity (MOE) of UF cover a wide range
92 (Clad 1964: 1070-2590MPa; Bolton and Irlle 1987: 3053-3743MPa). Therefore
93 the used adhesive was mechanically characterized by compression tests on
94 5x5x5mm sized cubes that were cautiously cured and conditioned to avoid
95 desiccation cracking. We measured a value of 3GPa for the UF adhesive used.

96 The frequency spectra of the samples were measured using a GRINDOSONIC
97 impulse excitation measuring device MK5. For this purpose, the boards were
98 placed on soft cellular plastic supports to minimize support-induced vibration of
99 the boards. The impulse was given by a small ball-hammer at the points indicated
100 in Figure 1c. Three different combinations of support setup and excitation location
101 were chosen to enhance distinct vibrational modes of the boards: One bending
102 oscillation each along the two small edges of the board and a torsion oscillation
103 (Figure 1c). The spectra are transformed using a Fast-Fourier-Transformation
104 (FFT) to extract the eigenfrequencies. After transformation, the signals of each
105 measurement are normalized to the maximum peak in order to allow identification
106 of the relevant modes.

107 The inverse determination of material properties consists of two parts: (i) The
108 extraction of eigenvalues of the Finite Element system Abaqus and (ii) an
109 optimization strategy to minimize the discrepancy between measured and
110 extracted eigenfrequencies. From the linearized equation of motion of a discrete
111 system with displacement vector u , namely

$$M\ddot{u} + Ku = p$$

112 for free vibration ($p=0$) and the harmonic ansatz for the displacements $u=\underline{u}e^{\omega t}$
113 leads to the Eigenvalue problem

$$(-\omega^2 M + K)\underline{u} = 0$$

114 with the global stiffness and mass matrix K and M , the eigenvector \underline{u} and the
115 angular frequency of the undamped oscillation ω . The non-trivial solution can be
116 found through

$$\det|\omega^2 M + K| = 0$$

117 However, direct determination of eigenvalues and respective eigenvectors of the
118 K, M matrix pair is not possible. A number of iterative methods like the Lanczos
119 eigensolver can extract eigenvalues from sparse symmetric systems (Argyris and
120 Mlejnek 1991). After extracting the eigenfrequencies f_n that correspond to the n
121 first bending and torsional modes, they are then compared to the experimental
122 values f_n^{exp} via an error function of the form

$$E_f(\%) = 100 * \sqrt{\sum_n w_n \left(\frac{f_n - f_n^{exp}}{f_n^{exp}} \right)^2}$$

123 with w_n as the weighting coefficient that is taken according to the accuracy of the
 124 experimental measurement for the respective frequency. This way it was assured
 125 that low frequencies that can be measured with high precision, are weighted
 126 higher ($w_n=0.2$) than higher eigenmodes ($w_n=0.1$), where the mapping of
 127 frequency to the respective mode is more difficult.

128 The underlying model has identical dimensions to the experiments and is
 129 discretized by volume elements with quadratic order (20 node brick element,
 130 C3D20R) but with reduced integration (Figure 1c). The plain wood is represented
 131 by an orthotropic material model, therefore by nine engineering constants E_R , E_T ,
 132 E_L , ν_{RT} , ν_{RL} , ν_{TL} , G_{RT} , G_{RL} , G_{TL} , and the density, all greater than 0. For each
 133 sample, the distance of the board center to the original tree center was
 134 determined, which then was introduced as the center of the cylindrical coordinate
 135 system of each model. As a first step the sensitivity of all material parameters on
 136 the first eigenfrequencies is studied.

137 Starting values for MOE and shear modulus (G) were chosen to cover the entire
 138 range given in literature (Table 1). For the density, the measured values were
 139 taken as starting values (Table 1). Since the Poisson ratio variations merely
 140 change eigenfrequencies, they are fixed to values of $\nu_{RT} = 0.59$, $\nu_{RL} = 0.028$, and
 141 $\nu_{TL} = 0.02$ (values taken from Kollmann and Cote 1968; Neuhaus 1981), reducing
 142 the parameter space to seven dimensions. We made a variation of one property
 143 at a time in between reasonable boundaries given in Table 1 with equidistant
 144 increments in between.

145 The sensitivity study revealed that basically for variations of the MOE (E_R , E_T , E_L),
 146 a change of the bending frequency modes can be observed, while the torsion
 147 ones remain constant. The opposite is found for G (G_{RL} , G_{RT} , G_{TL}). Note that the
 148 important conditions for orthotropic materials, namely

$$|\nu_{LR}| < (E_L/E_R)^{1/2}, |\nu_{LT}| < (E_L/E_T)^{1/2}, |\nu_{RT}| < (E_R/E_T)^{1/2},$$

$$1 - \nu_{LR}\nu_{RL} - \nu_{RT}\nu_{TR} - \nu_{LT}\nu_{TL} - 2\nu_{RL}\nu_{TR}\nu_{LT} > 0$$

149 are always fulfilled. For each variant, the eigenfrequencies are calculated and the
 150 value of the error function is calculated using the experimentally determined
 151 frequencies. The value that produces the lowest error is chosen, and taken as the
 152 input value for the calculation of the next engineering constant. Thus, the values
 153 for the seven mechanical properties change in every completed cycle and, at the
 154 end of the ten cycles, the set of variables that optimize the error function is
 155 obtained. These values are introduced as initial parameters to the refinement
 156 stage. The refinement works in the same way, but instead of using upper and
 157 lower bounds with 10 steps in between, now all the values are allowed to vary +/-
 158 10% in 20 steps.

159 To calculate the eigenfrequencies of the adhesive covered boards, the model is
 160 extended by two layers with C3D20 elements of thickness δ . Their material is

161 considered to be isotropic with fixed Poisson ratio (0.3) but variable MOE,
162 density, and δ (for ranges see Table 1). Optimal values are found using the
163 identical procedure as described above.

164 **3. Results and Discussion**

165 From the huge number of eigenmodes, only six, namely the first two uniaxial
166 bending and pure torsion modes, were selected (see Figure 2a), since those
167 could be identified reliably, due to the experimental equipment used. The second
168 bending mode along the radial direction ($\text{Bend}_{\text{rad}} 2$) however, proved to be
169 difficult to detect with the applied set-up. However when higher modes could
170 occasionally be clearly identified, they were used for the optimization as well. The
171 relative difference between the respective experimental and numerical
172 eigenmodes is less than 2.25%.

173 In Table 1 the resulting material parameters for the clear wood boards are
174 summarized. Note that they are in between known bounds from literature. As the
175 boards' dimension in the tangential direction was much smaller than in the radial
176 one, values for tangential direction cannot be found via inverse parameter
177 identification, but are also insignificant for this work.

178 **Table 1**

179 In Figure 2b, the shift of the respective modes due to the adhesive is shown. It is
180 striking that the bending mode in the radial direction changes most significantly.
181 As the MOE of the boards in this direction is much smaller than in the longitudinal
182 one, the adhesive layer has a higher influence on the MOE and therefore on the
183 radial bending modes. An example of the frequency spectra with and without
184 adhesive layer is given in Figure 2c.

185 **Figure 2**

186 The resulting, inversely identified effective parameters of the adhesive layers are
187 given in Table 1. It is interesting to find the effective MOE that lies in between the
188 values of pure wood in the radial direction and the pure adhesive.

189 **Conclusions**

190 With the proposed method it was possible to detect the eigenfrequency shifts
191 caused by the application of an adhesive layer on clear spruce wood boards. Via
192 inverse parameter identification, an estimate for the effective bond line properties
193 can be made, that are needed for simulation purposes. All values are within
194 reasonable ranges known from literature, showing the potential of the proposed
195 approach. However several improvements could be made for future studies:

- 196 • With a more sophisticated setup, based for example on laser vibrometry,
197 the eigenmode detection would be more accurate.
- 198 • With a quadratic board surface shape, overlapping modes should be
199 avoided.

- 200 • To reduce the parameter space, mechanical tests would be helpful. This
201 would be feasible by simple tension tests on strips produced from the
202 boards. Bending tests would only be possible in the longitudinal wood
203 direction since, as in the radial direction, the early wood section would
204 falsify the results.

205 **Acknowledgements**

206 Funding by the SNF- fund 200020_132662 Micromechanics of bondline failure and
207 CRSI22_125184 Multiscale analysis of coupled mechanical and moisture behavior of
208 wood as well as the provision of the adhesives by the companies Purbond/CH and
209 Geistlich Ligamenta/CH is acknowledged.

210 **References**

- 211 Argyris J and Mlejnek HP (1991) Dynamics of structures. North-Holland, Amsterdam
- 212 Berner M, Gier J, Scheffler M, Hardtke HJ (2007) Identification of material parameters of
213 wood and wood based panels by means of modal analysis. Eur J Wood Wood Prod
214 65(5): 367-375
- 215 Bodig J and Jayne BA (1982) Mechanics of wood and wood composites. Van Nostrand
216 Reinhold, Malabar (Florida)
- 217 Bolton AJ and Irle MA (1987) Physical Aspects of Wood Adhesive Bond Formation with
218 Formaldehyde Based Adhesives .1. The Effect of Curing Conditions on the Physical-
219 Properties of Urea Formaldehyde Films. Holzforschung 41(3): 155-158
- 220 Clad W (1964) Über das Wesen einer Verklebung und die Fugenelastizität ausgehärteter
221 Leimfugen bei Holzverleimungen. Dissertation, TH Stuttgart
- 222 Clauss S, Dijkstra DJ, Gabriel J, Kläusler O, Matner M, Meckel W, Niemz P (2011)
223 Influence of the chemical structure of PUR prepolymers on thermal stability. Int J Adhes
224 Adhes 31(6): 513-523
- 225 Habenicht G (2006) Kleben; Grundlagen, Technologien, Anwendungen. Springer Verlag,
226 Berlin, Heidelberg, New York
- 227 Hass P, Wittel FK, Mendoza M, Stampanoni M, Herrmann HJ, Niemz P (2011) Adhesive
228 penetration in Beech wood: Experiments. Wood Sci Technol 46 (1): 243-256
- 229 Kamke FA and Lee JN (2007) Adhesive penetration in wood - a review. Wood Fiber Sci
230 39(2): 205-220
- 231 Keunecke D, Sonderegger W, Pereteanu K, Lüthi T., Niemz P (2007) Determination of
232 Young's and shear moduli of common yew and Norway spruce by means of ultrasonic
233 waves. Wood Sci Technol 41(4): 309-327
- 234 Kollmann F and Cote WA (1968) Principles of Wood Science and Technology 1: Solid
235 Wood. Springer, Berlin, Heidelberg
- 236 Konnerth J and Gindl W (2006) Mechanical characterisation of wood-adhesive interphase
237 cell walls by nanoindentation. Holzforschung 60(4): 429-433

- 238 Konnerth J, Harper D, Lee SH, Rials TG, Gindl W (2008) Adhesive penetration of wood
239 cell walls investigated by scanning thermal microscopy (SThM). *Holzforschung* 62(1): 91-
240 98
- 241 Konnerth J, Jäger A, Eberhardsteiner J, Müller U, Gindl W (2006) Elastic properties of
242 adhesive polymers. II. Polymer films and bond lines by means of nanoindentation. *J Appl*
243 *Polym Sci* 102(2): 1234-1239
- 244 Neuhaus FH (1981) Elastizitätszahlen von Fichtenholz in Abhängigkeit von der
245 Holzfeuchte. Dissertation, Ruhr-Universität Bochum
- 246 Niemz P (1993) Physik des Holzes und der Holzwerkstoffe. DRW-Verlag, Leinfelden-
247 Echterdingen
- 248 Suchsland O (1958) Über das Eindringen des Leimes bei der Holzverleimung und die
249 Bedeutung der Eindringtiefe für die Fugenfestigkeit. *Eur J Wood Wood Prod* 3: 101-108
- 250

251 **Figures**

252 **Figure 1:** (a): Information flow between experiment and model. (b): Example for the
253 determination of the UF-bondline geometry in spruce. (c): Experimental setup variants
254 and mesh used in the simulations for the spruce wood samples with brick elements.

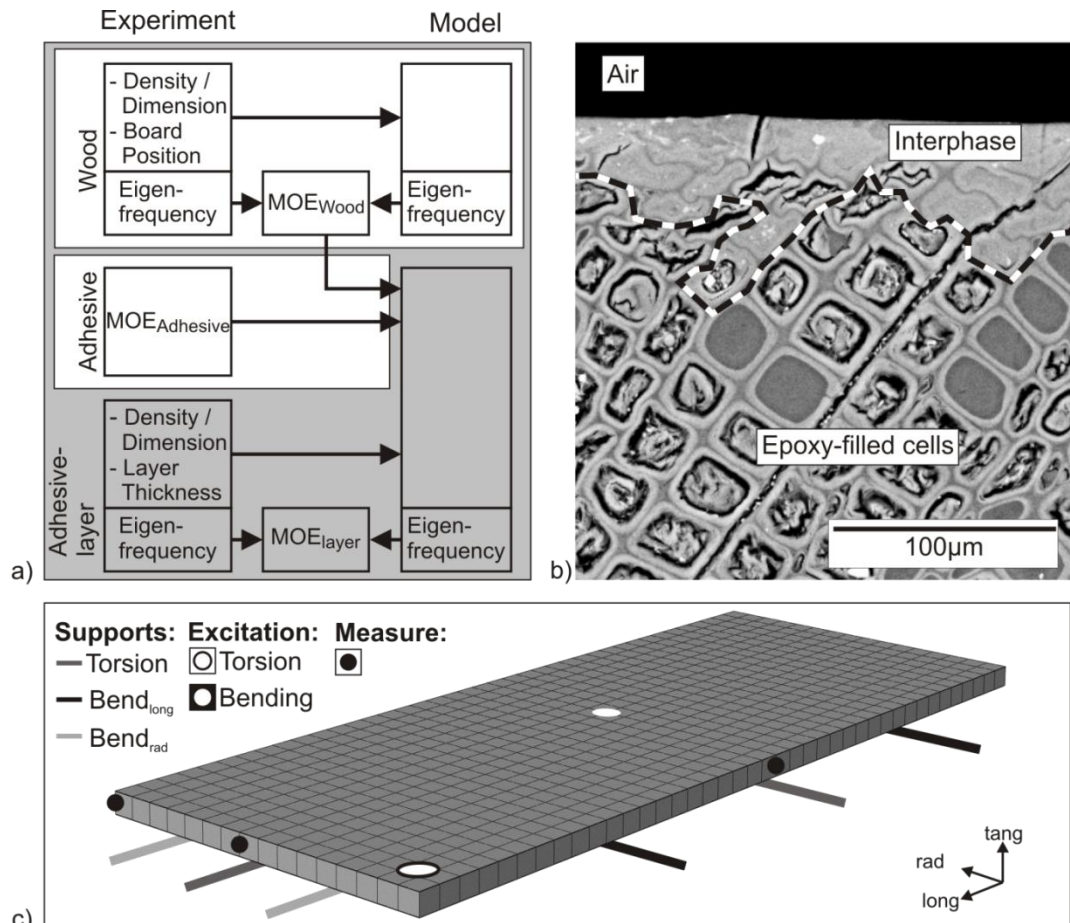
255 **Abbildung 1:** (a): Informationsaustausch zwischen Experiment und Model. (b): Beispiel
256 für die Bestimmung der Geometrie einer UF-Klebfuge in Fichte. (c): Experimenteller
257 Versuchsaufbau und Gitter für die Simulation der Fichtenproben.

258

259 **Figure 2:** (a): Denotation of eigenmodes, which were used for comparison between clear
260 wood samples and samples covered with adhesive layer. (b): Relative frequency shift in
261 the single modes caused by the adhesive application. (c): Example of eigenmode-
262 identification in clear spruce wood boards before and after application of UF adhesive
263 layers. Shown are representative frequency bands, measured using different
264 measurement setups, enhancing torsion and bending modes (see Figure 1c).

265 **Abbildung 2:** (a): Bezeichnung der Eigenmoden, die zum Frequenzvergleich zwischen
266 unbeschichteten und beschichteten Fichtenholzproben genutzt wurden. (b): Relative
267 Frequenzverschiebung in den einzelnen Moden durch die Beschichtung mit Klebstoff. (c):
268 Eigenmode-Identifikation an einem Beispiel vor und nach der Beschichtung mit UF-
269 Klebstoff. Abgebildet sind repräsentative Frequenzbänder; unterschiedlicher
270 Versuchsaufbau zur Verstärkung der Torsions- und Biegemoden (s. Abbildung 1c).

271



272

273

274

275

276

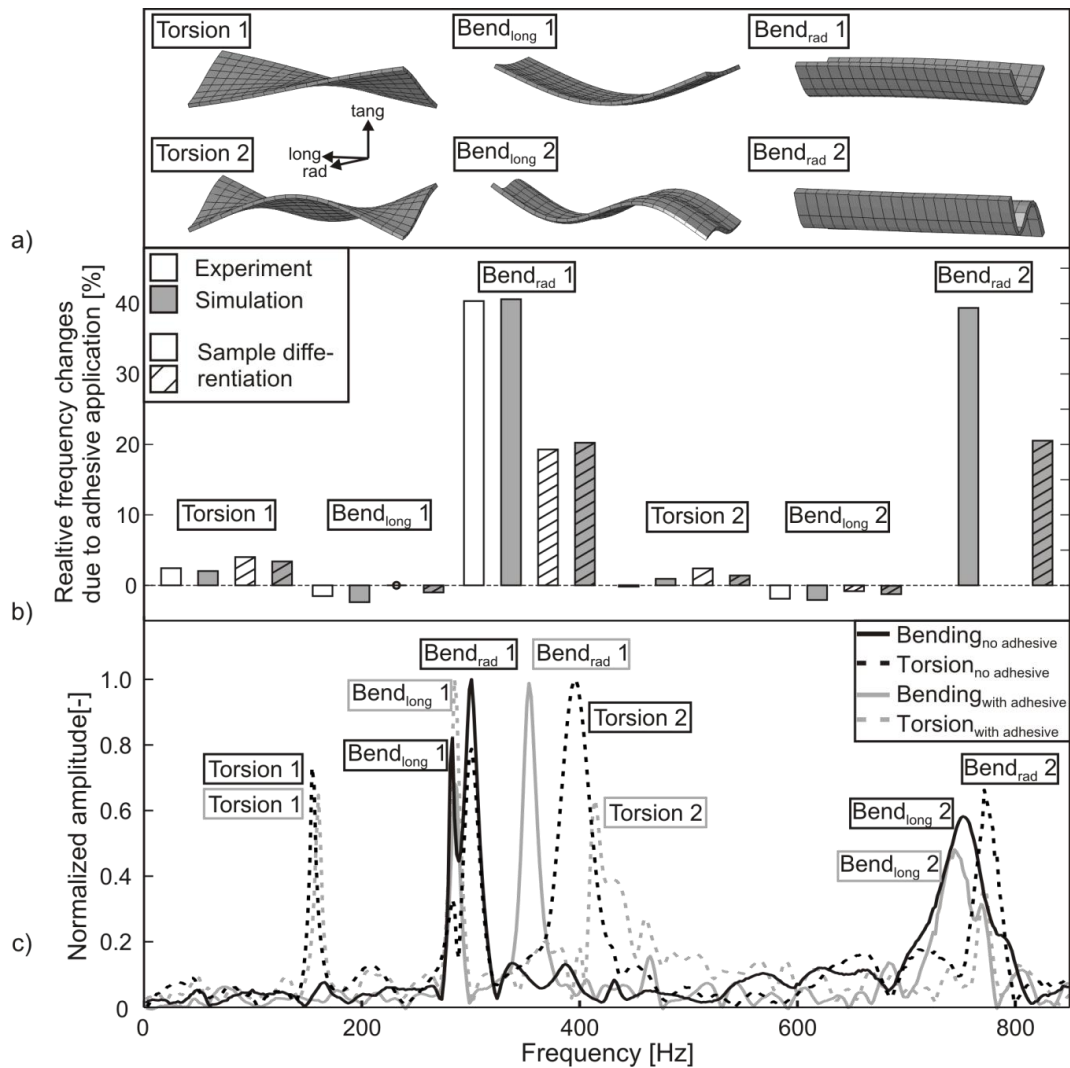
277

278

279

Figure 1: (a): Information flow between experiment and model. (b): Example for the determination of the UF-bondline geometry in spruce. (c): Experimental setup variants and mesh used in the simulations for the spruce wood samples with brick elements.

Abbildung 1: (a): Informationsaustausch zwischen Experiment und Model. (b): Beispiel für die Bestimmung der Geometrie einer UF-Klebfuge in Fichte. (c): Experimenteller Versuchsaufbau und Gitter für die Simulation der Fichtenproben.



280

281 **Figure 2:** (a): Denotation of eigenmodes, which were used for comparison between clear
 282 wood samples and samples covered with adhesive layer. (b): Relative frequency shift in
 283 the single modes caused by the adhesive application. (c): Example of eigenmode-
 284 identification in clear spruce wood boards before and after application of UF adhesive
 285 layers. Shown are representative frequency bands, measured using different
 286 measurement setups, enhancing torsion and bending modes (see Figure 1c).

287 **Abbildung 2:** (a): Bezeichnung der Eigenmoden, die zum Frequenzvergleich zwischen
 288 unbeschichteten und beschichteten Fichtenholzproben genutzt wurden. (b): Relative
 289 Frequenzverschiebung in den einzelnen Moden durch die Beschichtung mit Klebstoff. (c):
 290 Eigenmode-Identifikation an einem Beispiel vor und nach der Beschichtung mit UF-
 291 Klebstoff. Abgebildet sind repräsentative Frequenzbänder; unterschiedlicher
 292 Versuchsaufbau zur Verstärkung der Torsions- und Biegemoden (s. Abbildung 1c).

293

294 **Tables**

295 **Table 1:** Summary of values for clear spruce wood, bulk UF adhesive and UF adhesive
296 layer from literature, own measurements and calculations.

297 **Tabelle 1:** Übersicht von mechanischen Eigenschaften von Fichte, UF-Klebstoff und
298 Klebstoffschicht aus Literatur, eigenen Messungen und aus Berechnungen.

299

300 **Table 1:** Summary of values for clear spruce wood, bulk UF adhesive and UF adhesive
 301 layer from literature, own measurements and calculations.

302 **Tabelle 1:** Übersicht von mechanischen Eigenschaften von Fichte, UF-Klebstoff und
 303 Klebstoffschicht aus Literatur, eigenen Messungen und aus Berechnungen.

Literature values							
Clear Wood						Bulk adhesive	Ref
Density ^a [kg/m ³]	MOE [MPa]			G [MPa]			MOE [MPa]
	L	R	T	LR	LT	RT	
399	11700 – 13800	1680 – 1800	618 – 1170	617 – 642	587 – 615	51 – 53	1
470	10000	800	450	600	650	40	2
	10163 – 12438	700 – 1069	386 – 710	610 – 856	590 – 787	51 – 97	3
	11605 – 16716	687 – 903	392 – 638	618 – 746	500 – 853	29 – 39	4
417	11933	803	412	733	612	41	5
							1070 – 2590
							3053 – 3743
Measured values							
Clear wood		Bulk adhesive					
Density ^a [kg/m ³]	Density ^a [kg/m ³]	MOE [MPa]	Thickness (st. dev) [μm]				
461	1100	3000	48 (22)				
442			57 (15)				
Value-range for first calculation step							
Clear wood				Adhesive layer ^c			
Density ^{a,b} [kg/m ³]	MOE [MPa]			Density ^a [kg/m ³]	MOE [MPa]	Thickness [μm]	
	L	R	T				
x*0.8 – x*1.2	7000 – 30000	300 – 2000	200 – 1500	500 – 3000	500 – 7000	10 –150	
	G [MPa]						
	LR	LT	RT				
	360 – 1080	300 – 900	21 – 61				
Calculated Values (FEM)							
Clear wood				Adhesive layer ^c			
Density ^a [kg/m ³]	MOE [MPa]		G [MPa]		Density ^a [kg/m ³]	MOE [MPa]	Thickness [μm]
	L	R	LR	RT			
478	13720	1164	911	45	1016	2567	71.5
440	14000	1326	601	41	792	2567	53.0

304 ^a Acclimatized at 20°C and 65% relative humidity;

305 ^bx stands for measured values of the respective sample;

306 ^cAdhesive layer consist of pure adhesive and wood-adhesive interphase;

307 ¹Keunecke, Sonderegger et al. 2007; ²Niemz 1993; ³Bodig and Jayne 1982; ⁴Kollmann
 308 and Cote 1968; ⁵Neuhaus 1981; ⁶Clad 1964; ⁷Bolton and Irlle 1987